Molecular dynamics and docking studies on potentially active natural phytochemicals for targeting SARS-CoV-2 Main Protease

Sandhya KS (drkssandhya@gmail.com)
University of Kerala https://orcid.org/0000-0002-3628-0521
Achuthsankar S. Nair
University of Kerala

Research Article

Keywords: SARS-CoV-2, COVID19, Phytochemicals, DOCKTHOR, LibDock, Molecular dynamics

Posted Date: March 25th, 2022

DOI: https://doi.org/10.21203/rs.3.rs-1465489/v1

Abstract

In this study, we screened eighty seven novel phytochemical compounds and identified the best for targeting the main protease (M^{pro}) receptor of SARS-CoV-2. Interestingly, the studied phytochemicals are present in four natural herbs namely, *Aegle Marmelos, Coleus Amboinicus, Aerva Lanta and Biophytum Sensitivum*. After categorizing all the phytochemicals based upon LibDock scores, we identified six compounds with scores over 120, namely, Ervoside, Epoxyaurapten, Epicatechin, Feruloyltyramine, Marmin and Aegelinosides B. Among them Aegelinosides B leads with a very high LibDock value of 142.50 (binding energy: -8.54 kcal/mol). We also made molecular dynamics simulations for the best six systems and explored their structural stability (RMSD), Cα fluctuations (RMSF), intermolecular hydrogen bond interactions, effect of solvent accessibility (SASA) and compactness (Rg) factors. Satisfactory ADMET and druglikeness features were found for all these compounds and we therefore strongly propose the initiation of trial studies on these compounds for fighting SARS-CoV-2.

1. Introduction

Controlling and defeating the deadly pandemic, COVID 19, is the most challenging issue the world is facing today. The work of Yan *et. al.* [1] provided the early understanding that “human angiotensin converting enzyme 2” (hACE2) is a potential receptor for SARS-CoV-2. The SARS-CoV-2 pathogen, once reached inside the lungs, easily gets attached with hACE2 and undergoes in-situ integration rapidly [2]. Reports reveal that SARS-CoV-2 can mutate its own protein structure upon human to human transmission [3]; as for example, P1 (B.1.1.28), SARS-CoV-2 VOC 202012/01 (B.1.1.7), 501Y.V2 (B.1.351) and B.1.617.2 are the four recent mutated fast spreading variants [4]. The world is striving hard for ensuring an absolutely effective and affordable vaccine is available at the earliest but the issues related with large scale production, affordability and global accessibility remain elusive [5, 6]. As far as the existing vaccines are concerned, still considerable skepticism exists regarding the improved immunity for humans without any risks of having complications after administration [7].

It is widely accepted that for fighting a new disease, adopting a “repurpose” strategy through commercially available drugs (e.g., antimalarial drugs, anti HIV protease inhibitors or interferon beta-1b, etc) can reduce the time and manpower [8]. With the help of computers one can screen virtually over millions of small molecules and also model the drug target known as “homology modelling” strategy. Several SARS-CoV-2 main protease (M^{pro}), PL^{pro}, RdRp, Nucleocapsid, Helicase and Spike protein have been reported experimentally which triggered screening of available drugs or small molecules using different molecular docking approaches [9]. Especially, M^{pro} plays a dominant role in the maturation of functional polypeptides involved in the viral replication and transcription, hence making it an attractive drug target for the development of COVID19 therapeutics [10]. Moreover, the crystal structure of M^{pro} contains several substrate binding sites, making it an opportunity for testing wide varieties of inhibitors. Lu studied the anticorona activities of four anti HIV protease inhibitor drugs namely, nelfinavir, pitavastatin, perampanel, and praziquantel and found that nelfinavir is the best for fighting SARS-CoV-2

[11]. In another study, Wang *et. al*.. reported that the FDA approved drugs such as chloroquine and remdesivir can be effectively used for fighting COVID-19 [12]. However, the preliminary studies have not yet been approved as a consolidated treatment strategy for the COVID-19 infected patients since many drugs have low efficiency level in terms of cure reports. Another important concern for many drugs is severe side effects after consumption, hence a best alternative option is to scrutinize the safe natural products for the treatment of COVID19. In view of this, phytochemicals receive considerable attention, as they are a rich source of several flavonoids, alkaloids, terpenoids, fibers, limonoids, glucosinolates, peptides, polyphenols etc. Good numbers of reports are available for the docking of small molecules extracted from Pubchem, ChEBI, ZINC, drug bank, CEMBL, chemspider, etc. Hasanain *et. al.* studied the molecular dynamicity of the real time movement of M^{pro} in the presence of Conivaptan and Azelastine ligands and found the best binding pockets of M^{pro} [13]. Large numbers of experiments and in-silico molecular docking studies were reported recently [14–16]. Goswami *et. al.* employed several FDA approved drugs for studying the anti corona activities and suggested that triterpene saikosaponin and simeprevir are potential inhibitors [17, 18]. Based on molecular docking study, Nigellidine and alpha Hederin compounds containing herbs were recently suggested as inhibitors for SARS-CoV-2 [18].

Many traditional herbs with Indian origin have been proven effective for cough, asthma and bronchitis [19]. Inspired by this, for the current study, we selected four different herbal species namely, *Aegle marmelos*, *Coleus Amboinicus*, Aerva Lanta and *Biophytum Sensitivum*. These herbs are being used as a first aid home remedy and especially it is abundantly available throughout Kerala state of India. The phytochemicals present in these herbs are well documented using various spectroscopic methods and reported in the literature [20–23]. Apart from that, these medicinal herbs are clinically proven for various pharmacological activities and now emerged as an unavoidable part for treating various life threatening infections. For instance, *Aegle marmelos* is proven for its anticancer, antipyretic, radioprotective and anti-inflammatory properties [24]. Aromatic perennial herb *Coleus Amboinicus* is used for malarial fever, colic, epilepsy and helminthiasis, etc [25]. *Aerva Lanta* is known for its anthelmintic, antibacterial, anti-inflammatory effects [26]. *Biophytum Sensitivum* exhibits excellent antioxidant, anti-inflammatory, anti cancer, anti diabetic and antioxidant activities [27, 28].

The main objective of the present work is to explore the best phytochemical constituents from four medicinal herbs for neutralizing M^{pro} and to understand the mechanism of its interaction. We identified 87 phytochemicals from these herbs and then screened them by performing docking study. For the best ranked phytochemicals, molecular dynamics simulation studies were performed. Subsequently the ADMET properties and drug likeness were analyzed and from these important insights were explored for drug design.

2. Materials And Methods

2.1 Preparation of Protein

The structure of SARS-CoV-2 M^{pro} was used as a receptor for the present study. The corresponding PDF ID: 6LU7 is downloaded from Protein Data Bank. The 3D crystal structure of M^{pro} with resolution, 2.17 Å consists of three domains (Domain I, II and III). with 8-101, 102–184 and 201–306 amino acid residues, respectively. Domain I and II consist of β-barrels while domain III mainly consists of α-helices. The active binding site is located at the cleft of domain I and II. The inhibitor N3 and water molecules were deleted from it. Visualization and docking were performed on licensed discovery studio software [29]. All pdb files were first opened by the discovery studio and then added polar hydrogen. The protein is minimized using CHARMm forcefield and smart minimizer algorithm with a maximum step of 2000. All these options were set to be default in discovery studio. Chimera software was used for visualization.

2.2 Preparation of ligand

Aegle Marmelos (in the local language of Kerala (Malayalam), it is called Koovalm) consists of 20 phytochemicals, whereas *Coleus Amboinicus* (Navara) contains 24 chemical constituents. Aerva lanta (Cherrula) and *Biophytum Sensitivum* (also known as little tree plant, in malayalam it is called as Mukkutti) consists of 17 and 26 phytochemicals, respectively. Chemical identity information of all these compounds were taken from the previously published literature[19] and the corresponding files were downloaded from ChEBI[30] and Pubchem[31] (the obtained files (totally 87) were in .sdf format, which needs to be converted to .dsf format). The phytochemicals were prepared by adding polar hydrogen and then minimized using input CHARMm forcefield with smart minimizer algorithm (maximum step: 2000. The RMS gradient was 0.01). The partial charge estimation is done by Momany- Rone method.

2.3 Druglikeness and ADMET analysis

The druglikeness of screened drugs was carried out by Lipinski rule of five and Veber rule as implemented in the Discovery studio. All compounds need to show molecular weight < 500g/mol, number of hydrogen donors < 5, number of hydrogen acceptors < 10 and AlogP98 < 5 and no more than one violation of above Lipinski rule criteria is permitted[32] Molecular weight of compounds greater than 500g/mol were avoided before analysis. Rotatable bond < 10 and polar surface area (PSA) < 140 and total hydrogen bond donors and acceptors < 12 are criteria for the Veber rule [33]. 87 candidates satisfied Lipinski rule criteria out of the 98 phytochemicals taken from the literature. Absorption, distribution, metabolism and excretion and toxicity (ADME/T) are the five pharmacokinetic properties of all drugs which must be checked out. Aqueous solubility, blood brain barrier penetration (BBB), cytochrome P450 inhibition (CYP250), hepatotoxicity, human intestinal absorption (ADMET absorption level) and plasma protein binding (PPB) are the ADMET properties calculated using the QSAR. Calculations were done under the calculated molecular properties protocol and ADMET properties tool. The ADME/T properties are given in the supporting information.

2.4 Molecular docking

Binding site of M^{pro} was first determined using the option tool "define and edit binding site" under "ligand receptor interaction" tool panel of discovery studio. The active site was chosen based on the location of co-crystallized peptide inhibitor N3. The spherical transparent binding sphere was created around the

centroid of the selected inhibitor and then taken for the binding site attribute. After preparation and minimization, binding site is defined for the docking of protein with ligands. In the process of molecular docking, the predicted active binding site radius is set to be 10 Å and centered at 12.355, 14.273, 71.259, XYZ coordinates for M^{pro} (Fig. 1). The aligning ligand conformations to polar and nonpolar receptor interaction site, also known as hotspot was done by high throughput virtual screening (HTVS) using LibDock protocol. Various parameters such as max conformation hit, final cluster radius, final score cut off and maximum BFGS were set to be default under high quality modes. LibDock protocol allows generating several modes of ligand conformations for docking. Number of Hotspot and docking tolerance are 100 and 0.25, respectively. LibDock score can be taken directly from the output files which are saved in .dsf format. Highest value of docking score and maximum number of hydrogen bonds are the two criteria for the selection of LibDock score.

2.5 Binding energy Calculation

All phytochemicals from each herb were converted into mol2 format. Protein must be in pdb format to be compatible with DOCKTHOR online server for binding energy calculations [34]. DOCKTHOR utilizes the multiple solution steady state genetic algorithms used for the search method. Here, we fix the same XYZ coordinate which is defined for the protein. The default grid box is 20 Å × 20 Å× 20 Å. Number of maximum evaluations is 500000 and number of runs is set to be 12. Soft docking is performed for the protein flexibility using MMFF94S Buf-14-7 potential. The output files obtained consist of top-ranking ligands with binding energy (kcal/mol). The binding results are given in the Table 2. Aegelinoside B Feruloyltyramine and Feruloyltyramine show binding energy (BE) greater than 8 kcal/mol. It is noted that LibDock score and DOCKTHOR server are consistent in their performance in terms of LibDock score and BE even though exceptions can be seen. Different algorithm used for the two methods could be the reason for the variation. Nonetheless, in general, highest LibDock values of chemical constituents are always seen with good BE obtained in DOCKTHOR.

2.6 Molecular dynamics simulations

The molecular dynamics (MD) simulations of top docked protein-ligand complexes were performed using WebGRo for macromolecular simulations. The server uses Gromacs protocol for carrying out many parameters such as RMSD, RMSF, ligand RMSD, Rg, SASA (total) total and M^{pro}-ligand hydrogen bond plots, total volume and density [35]. The force file was GROMOS96 43al applied for all six top docked complexes. The ligand topology was created by the PRODRG tool. TIP4P was selected as a solvent model with triclinic box. The system was neutralized by adding 33 sodium and 29 chlorine ions (0.15 M salt) based on the total charges. The steepest descent algorithm with 5000 steps was applied for energy minimization. For equilibration and MD run parameters were set at 300 K and pressure, 1 bar. Modified Berendsen thermostat named V-rescale was used for temperature coupling. The MD integrator was set to be of leaf frog method for updating position and velocities. MD simulation was performed for 100 ns with approximate number of frames, 5000 per simulation. Three replica simulations per system were

performed in order to ensure the reproducibility. First set calculations were discussed in the text and remaining plots were shown in supplementary information [SI].

3. Results And Discussion

A brief summary of four herbs (*Aegle Marmelos, Coleus Amboinicus, Aerva Lanta* and *Biophytum Sensitivum*) referred for the present study and their biological / therapeutic value are given in Table 1. Initially by using molecular docking study we scrutinized 87 phytochemicals obtained from these herbs for finding the most effective among them. Out of these 87 constituents, appreciable LibDock scores can be obtained for Aegelinoside B, Ervoside, Epoxy aurapten, Epicatechin, Feruloyltyramine, Marmin, Anhydromarmeline and Quercetin. Moreover, the corresponding binding energies are also found to be greater than 7.5 kcal/mol. The highest LibDock score of 142.50 is observed for Aegelinoside B. Ervoside and Epoxyaurapten exhibit next best dock score values of 129.69 and 129.06 respectively. List of phytochemicals with LibDock score > 120 and their corresponding binding energy values are shown in Table 2. Complete details of all these compounds are given in the supporting information (SI). Reference compounds such as Rimonabant, Metixene, Remdesivir, Indinavir, Oxiconazole, Doxapram, Pirenepine, Pimozide, Zopiclone, Saquinavir and Tipranavir were taken for comparison [36, 37]. It can be noted that Aegelinoside B exhibit higher LibDock score than some of the popular compounds reported in the literature, such as, Rimonabant, Metixene, Oxiconazole, Doxapram, Pimozide, Zopiclone, Saquinavir and Tipranavir. Among these, Remdesivir shows a closely competitive LibDock score as compared to our study (Indinavir is the second highest). Detailed descriptions are provided in the following subsections, 3.1–3.6. From the present reference compounds, Remdesivir is the only FDA approved nucleoside COVID19 drug which inhibits the replication of RdRp of SARS-CoV-2 by terminating its chain [38]. Others are repurpose drugs used for other viral infections and some of them are used to conduct computational studies for docking purposes [39–42].

Table 1
Medicinal and physiological properties of herbal plants considered in the current study.

Medicinal plants	Family	Action
Aegle marmelos	Rutaceae	Stomachic, asthma, antimicrobial (specific for diarrhoea, colitis, dysentery and enteric infections), digestive, astringent, spasmolytic,antiallergic activity, hypoglycaemic.
Aerva lanata	Amaranthaceae	Anticalculus (used in lithiasis), lithontriptic, diuretic, demulcent, anthelmintic, antidiarrhoeal, anticholerin, bechic; leaf used in headache and hepatitis, root in strangury.
Biophytum sensitivum	Oxalidaceae	Insomnia, strangury, asthma, phthisis, diabetes, convulsions, cramps, chest-complaints, inflammations, tumours, stomachache, diuretic, astringent, antiseptic, chronic skin diseases.
Coleus Amboinicus	Lamiaceae	Epilepsy and other convulsive affections, asthma, bronchitis, cold and chronic cough, urinary diseases, vaginal discharge, colic and dyspepsia. Stimulates the function of liver.

Table 2
Summary of phytochemicals with LibDock values and Binding energies.

Plants	Phytochemicals	LibDock	BE in kcal/mol
Aegle marmelos	Aegelinoside B	142.50	-8.54
	Epoxyaurapten	129.06	-7.75
	Marmin	122.66	-7.84
Biophytum sensitivum	Epicatechin	124.33	-7.69
Aerva lanata	Ervoside	129.69	-7.91
	Feruloyltyramine	123.22	-8.01

3.1 Docking analysis of the phytochemical constituents from *Aegle Marmelos*

The obtained binding energy for the complex structures from this category (phytochemicals of *Aegle Marmelos* docked with M^{pro}) ranges from − 8.55 kcal/mol to -7.14 kcal/mol. For these the LibDock score is between 142.00 to 63.00. Tigogenin (-8.55 kcal/mol), Aegelinoside (-8.54 kcal/mol) and Dehydromarmeli (-8.53 kcal/mol), show best binding energies obtained from DOCKTHOR. O-Prenylhalfordinol, Imperatorin, Skimmianine, N-[2-Ethoxy-2-(4-methoxyphenyl)ethyl]cinnamide, Xanthotoxin, Aeglemarmaelosine, Anhydromarmeline and Aegeline exhibit binding energy values between − 8.41 kcal/mol to -8.06 kcal/mol. Umadevi *et. al.*[43] reported a binding energy value of -7.2 kcal/mol for Imperatorin-M^{pro} complex (also known as Marmelosin) obtained from autodock which is lower than that

obtained from the current study (-8.39 kcal/mol). Aegelinoside B, an alpha glucosidase inhibitor, is the phytochemical that can be extracted from the leaves of *Aegle marmelos*. The 3D interaction diagram shown in Fig. 2A indicates the hydrogen bond donors and hydrogen bond acceptors around Aegelinoside B. We have observed that Aegelinoside B interacts with GLU166, GIN192, THR190, ARG 188 and GLN189 through conventional hydrogen bonds. The hydrogen of GLN 192 interacts with two O3 and O5 of the ligand, while oxygen of THR 190 residue interacts with H35 and H34 of ligands. Altogether seven hydrogen bonds can be seen in the 2D figure (Fig. 2B). Numerous carbon-hydrogen bonds and two π-sulphur interactions, one π-π stacked and one π alkyl interactions can be observed. The hydrogen bond interactions of native ligands (Inhibitor N3) in the crystal structure showed GLY143, GLU166, HIS164, PHE140, GIN 189 and THR 190. However, the docking studies on the native ligand with M^{pro} reveals that hydrogen bond interactions involving the residues are HIS41, HIS163, HIS172, GIN189, THR190 and GLU166. The common hydrogen bond interacting residues are GLU166, THR190 and GIN189. Such interactions are also observed on the Aegelinoside B with M^{pro} in our docking results. The other important constituents of *Aegle marmelos* that exhibit good LibDock scores are shown in the Table 2. The second best scored (129.06 kcal/mol) complex, Epoxyaurapten is shown in the Fig. 3. It forms four hydrogen bonds with ASN142 (here, two hydrogen bonds), THR190 and GLU166. π- anion interactions were found between GLU166 and the aromatic part of the ligand and other π- alkyl interactions can be seen with CYS145 and HIS41. The third best, Marmin, exhibits 4 hydrogen bonds (Fig. 4). The hydrogen bonded interacting residues in this case are, TYR54, GLU166, GLY143 and SER144. GLY143 is the common active residue seen in Epoxyaurapten and Aegelinoside B whereas GLU166 active interacting residue can be seen in all three complexes and the native ligand. For further understanding, molecular dynamics (MD) studies were performed for Aegelinoside B, Epoxyaurapten and Marmin, and the results are highlighted in section 3.6.

3.2 Docking of the phytochemicalconstituents from *Aerva lanata*

Aerva lanata contains many alkaloids and flavonoids and hence is quite popular for various biological activities. It is used for antiurolithiatic, astringent, diuretic, antimicrobial, anti-inflammatory and hepatoprotective drugs. One of the major chemical constituents of Aerva lanta is Ervoside, which is a biologically active canthin-6-one alkaloid [44]. Our study reveals that, out of 17 phytochemicals obtained from *Aerva lanata*, Ervoside docks better with M^{pro} target, with a LibDock score of 129.69 kcal/mol (Fig. 5). The TYR54, HIS172, CYS145, SER144 and MET165 residues interact with Ervoside through hydrogen bonds. A sulphur π- interaction can be seen for MET49 residue. The second best Libdock scored (123.22) phytochemical is Feruloyltyramine. This compound contains three hydrogen bonds with the protein (Fig. 6). The active residues of M^{pro} are ASP776 and THR556. It is interesting to note that the binding site is slightly changed and due to this reason common active residues have not involved in the interaction. Methergine, Ervolanine, Kaempferol, Quercetin and 4-Methoxykaempferol exhibit LibDock score in the range of 110 to 130 kcal/mol. Interestingly, Quercetin has been studied for protective effects from COVID19 induced acute kidney injury [45]. In our study, Quercetin shows five Hydrogen bonds with

GLY143, SER144 ARG and MET165 residues while GLY143 and SER144 residues make three hydrogen bonds with Kaempferol. Even though higher number of hydrogen bonds seen in Qucercetin, it appears that the LibDock score is close to the score of Feruloyltyramin. In this category, we have selected best two phytochemicals based on the LibDock score. Hiremath *et. al.* reported in-silico docking analysis of Kaempferol and Quercetin obtained from the leaves of phyllanthus amarus. The binding affinity of these compounds with M^{pro} in their study was − 7.70 kcal/mol and − 7.50 kcal/mol, respectively [46]. DOCKTHOR provides closely similar binding energies of -8.10 kcal/mol for Kaempferol and − 7.97 kcal/mol for Quercetin. However, Kaempferol with spike protein indicates a significant improvement in binding affinity (-9.6 kcal/mol) [46]. Proceeding with the docking studies, MD studies were also performed by us for Ervoside and Feruloyltyramine, and the results are highlighted in section 3.6.

3.3 Docking of the phytochemical constituents from *Biophytum sensitivum*

Maximum number of phytochemicals is seen for *Biophytum Sensitivum* harbs, however most of them exhibit binding energy values less than − 7 kcal/mol. Attractive among them is Epicatechin which exhibits a LibDock score of 124.33. Reports indicate that Epicatechin mediates reverse transcriptase inhibiting activity for HIV [47, 48]. The green tea also contains Epicatechin and its derivatives such as, epigallocatechin gallate epicatechin gallate and gallocatechin-3-gallate. These compounds and their interactions with M^{pro} were studied previously by Ghosh *et. al.* [49]. The binding energy of Epicatechin was found to be -7.20 kcal/mol which is similar to our estimation (-7.69 kcal/mol). The hydrogen bond interactions occurred between HIS164, HIS163, SER144, PHE140 and ASN142 residues with the ligand. Numerous van der Waals and two π alkyl interactions can also be seen in Fig. 7. The other phytochemical is Stigmast-4-en-3-one, which exhibits a LibDock score of 118.74. It has only two hydrogen bonds between SER144 and HIS163 residues with oxygen ligands. Gamma Sitosterol and 4-hydroxy-3,5-dimethoxy hydrazid Benzoic acid have shown similar LibDock scores of 111.12 and 111.15, respectively. However, Dicyclohexyl phthalate, Gamma Sitosterol and Stigmast-4-en-3-one show a binding energy value greater than − 8 kcal/mol. The exact values observed for Dicyclohexyl phthalate, Gamma Sitosterol and Stigmast-4-en-3-one, respectively, -8.84 kcal/mol, -8.47 kcal/mol and − 8.31 kcal/mol. The M^{pro} – Epicatechin complex was further explored by MD study and the results are provided in section 3.6.

3.4 Docking of the phytochemical constituents from *Coleus Amboinicus*

Coleus Amboinicus is also known as Indian borage and is used for respiratory diseases like sore throat, cold, bronchitis, asthma, etc [50]. Recent studies indicate its antiproliferative effect against cancer cell lines [51]. Maste and Saxena studied the possibility of multi target response of the chemical constituents of *Coleus Amboinicus* [52]. They considered only four ligands and all these exhibit less than − 8.00 kcal/mol which agrees well with our observations. Here, we considered a maximum of 24 chemical constituents. None of the phytochemicals of the *Coleus Amboinicus* plant except N-benzoyl-L-

phenylalaninol show > 100 LibDock score and > -8 kcal BE. Among all the phytochemical constituents from this set, only N-benzoyl-L-phenylalaninol shows a highest binding energy of -8.22 kcal/mol. However, as compared to chemical constituents of the other three herbs, our observation is that the docking values are not high enough. Only N-benzoyl-L-phenylalaninol exhibits over 100 LibDock score. Conventional hydrogen bonding occurs between residue GLN189 and two OH and NH bonds from the ligands and residue GLU 166 with O of N-benzoyl-L-phenylalaninol. None of the constituents are attractive candidates for the further studies since most of them show less than LibDock score of 100 (except two candidates showing LibDock score of 111 and 104). Hence, no compound in this section was subjected to MD study.

3.5 Druglikeness and ADMET screening

Assessment of Lipinski rule and pharmacokinetics are important for optimizing drugs [30]. Owing to toxicity, many drugs fail at clinical trial stage, hence it is necessary to find lead compounds with good pharmacokinetics properties [53]. Lipinski rule, also known as rule of thumb, is an algorithm based model which predicts the drug likeness of small molecules. In this study, 87 constituents did not violate more than one criterion. Stigmast-4-en-3-one and Gamma Sitosterol display highest lipophilicity (8.319 and 8.084, respectively) whereas (13R)-8,13-epoxylabd-14-ene, Aurapten and 3-Methoxyamphetamine are in the border line. Only 3-Hydroxy-4-methoxybenzoic acid violates the Veber rule (PSA 2D of 151.42) whereas the remaining compounds were accepted as oral bioavailability of potential drugs by means of Veber's rule.

Compounds were scrutinized for their pharmacokinetic properties and toxicity using in-silico method as implemented in Discovery studio. After administrations all the phytochemicals show good absorption and moderate absorption except 3-Hydroxy-4-methoxybenzoic acid, Gamma Sitosterol and Stigmast-4-en-3-one. Bioavailability of drugs depends on the solubility level and the majority of the constituents tested in this study exhibits good and optimal solubility in water at 25°C. (13R)-8,13-epoxylabd-14-ene, Tigogenin, Gamma Sitosterol exhibit very low solubility. BBB model describes the blood brain barrier penetration level of the drug to the central nervous system of the brain and spinal cord. Note that, small lipophilic potential drug molecules should enter the nervous system and stay there a long time for the desired action. In this study, majorities of drugs are in very high, high, medium and low level of BBB except those for 4',7-Dimethoxykaempferol, Gamma Sitosterol, Stigmast-4-en-3-one, 3-Hydroxy-4-methoxybenzoic acid, dl-Phenylephrine, Ervoside and Methoxykaempferol. Aegelinoside B is at the border level and all constituents are non-inhibitors except Aeglemarmaelosine, oct-1-en-2-ol and 3-Butylindolizidine. Eight, twelve, eight and eleven constituents of *Coleus Amboinicus*, Aerva Lanta, *Aegle Marmelos* and *Biophytum Sensitivum*, respectively, are toxic in nature. The binding of a drug with plasma protein was described using PPB Tight binders, as shown by 49 compounds (< 1) remaining indicating the weak binders. Gamma Sitosterol, Anhydromarmeline and Stigmast-4-en-3-one show a value of greater than 7. All the well docked ligands are acceptable as a drug in terms of pharmacokinetics. All chemical constituents provided in the SI exhibits good druglikeness and pharmacokinetics properties.

3.6 Molecular dynamics simulation

In order to evaluate the stability of ligand bound protein, conformations, flexibility and compactness, we also performed MD simulations. For this, we selected the top six ligand docked protein complexes with M^{pro} and also evaluated the ligand induced changes on the protein structure. Figure 8A represents the root-mean-square deviation (RMSD) profile of docked complexes, which indicates the stability of the protein ligand complex. RMSD values were gradually increased till 7 ns time scale except Epicatechin, which stabilized quickly after about 4 ns for the first run. Proteins with Aegelinosides B, Ervoside, Feruloyltyramine, Epicatechin and Marmin were quite rigid with RMSD < 0.45 nm after 17 ns. On the other hand, Mpro-Epoxyaurapten complex show rigidity with RMSD < 0.55 nm. Initially all complexes with ligands were flexible in nature and then they reached a stable state. Epicatechin bound complex show some marginal fluctuation compared to others in the first run. However, it attains stability quickly in second and third run simulation (SI). Three replicas of MD simulation have been performed for the all six docked protein complexes for 100 ns. All complexes show a similar trend in RMSD for at least two run simulations whereas, Epoxyaurapten and Marmin exhibit similar RMSD plot for three replica calculations. The complexes achieved stability after 25 ns (SI). We observed that this system is highly stable as compared to the Mpro-Lopinavir complex [54]. The average RMSD values for M^{pro}-Aegelinoside B, M^{pro}-Ervoside, M^{pro}-Epoxyaurapten, M^{pro}-Epicatechin, M^{pro}-Feruloyltyramine, M^{pro}-Marmin and M^{pro} were found to be 0.32 nm, 0.31 nm, 0.339 nm, 0.390 nm, 0.327 nm, 0.310 nm and 0.320 nm, respectively. In general, it can be said that all complexes attain good stability and similar behavior till the end of the simulations. RMSD of ligands as a function of simulation time is plotted (Fig. 8B) and it indicates that all ligands are located well within the active site of protein. All ligands rapidly reached the dynamic equilibrium after 20 ns. Feruloyltyramine shows a small increment in RMSD (0.3 nm) after 7 ns and then reaches an earlier equilibrium state after 13 ns. In the case of Aegelinoside B, a dynamic equilibrium persists up to 15 ns and thereafter shows many fluctuations in RMSD. It can be suggested that Marmin adopted a small change in the conformation, but later on it reverts to stable state [55]. Similar case is also possible for the conformational change of Epoxyaurapten. Remaining ligands show minimal fluctuations and they maintained RMSD value within 1 nm till the end of MD simulation. Epicatechin and Feruloyltyramine show lowest fluctuations as compared to other ligands, indicating the highest stability of the simulation system [56].

The root-mean-square fluctuation (RMSF) of Cα carbon atoms for M^{pro} and M^{pro}-Ligands was estimated for analyzing the flexibility of residues of protein (Fig. 9). A significant fluctuation has been seen in the region of residue THR169 of M^{pro}-Epoxyaurapten and M^{pro}-Epicatechin. The RMSF value of these complexes is 0.42 nm and the corresponding residue is one of the pocket atoms having no interaction with ligands. M^{pro}-Epicatechin also shows a strong RMSF fluctuation at MET6 and LYS12 in comparison to other complexes. Another strong fluctuation (RMSF = 0.40 nm) was observed for M^{pro}-Aegelinoside B and M^{pro}-Marmin of residue ASN142. The residue of ALA193 fluctuations in M^{pro} was not observed for M^{pro}-Aegelinoside B, M^{pro}-Epicatechin, M^{pro}-Epoxyaurapten, M^{pro}-Marmin and M^{pro}-Ervoside. The average value of RMSF for M^{pro} and all complexes are in the range of 0.15 nm to 0.20 nm. Residues of complex of protein with Epoxyaurapten, Epicatechin, Feruloyltyramine and Marmin did not show much flexibility in

comparison to M^{pro} for at least two run [SI]. Hence, these complexes could be regarded as stable systems.

In addition, we evaluated the intermolecular hydrogen bonds formed between protein and ligands during the simulation. In fact, H-bond is a main factor in determining selectivity, stabilization and binding affinity. The M^{pro}-Aegelinoside B contains a maximum of five hydrogen bonds, out of which two hydrogen bonds were consistently seen during the simulation. Moreover, within 0.35 nm we identified a maximum of 8 hydrogen bonds. M^{pro}-Epicatechin, M^{pro}-Epoxyaurapten, M^{pro}-Ervoside, M^{pro}-Feruloyltyramine and M^{pro}-Marmin contains an average of 1, 1, 2, 2, and 1 hydrogen bonds, respectively, for MD runs (SI). The constant range of intermolecular hydrogen bonding of M^{pro}-Epoxyaurapten persists throughout the simulation indicating highest stability compared to other ligands and no change in the conformation [57]. Solvent accessible surface area (SASA) and radius of gyration (Rg) are used to analyze solvent accessibility of all complexes and structural compactness of protein. We observed that the average value of Rg for M^{pro} and M^{pro}-Marmin has almost similar Rg value (2.13 nm) and others show values in the range of 2.10 to 2.16 nm for three MD run. M^{pro}- Feruloyltyramine (Rg = 2.15 ns) shows highest Rg and this suggests slightly less compactness in comparison to other complexes and free M^{pro} (Fig. 10A). *Khan et. al.* reported that Remdsivir, Saquinavir and Darunavir provide average Rg score values (2.2 ± 0.1 nm) which are at the upper range of obtained score of our drugs (2.10 nm – 2.16 nm) [58]. M^{pro}-Epoxyaurapten shows highest compactness and stable folding due to being lowest in the Rg value, which was maintained till the end of the simulation for three MD runs [59]. Moreover, Rg of all complexes decrease over the simulation time (SI), meaning that binding of ligands helps stabilization of the whole complex [60]. The effect of solvent molecules on the residues of M^{pro} when it is bound with ligand is confirmed from SASA versus MD simulation time. All M^{pro}-Ligands complexes and M^{pro} show SASA values in the range of 115 nm^2 to 145 nm^2 (Fig. 10B). For M^{pro}-Marmin, a decrease in SASA value in comparison to other complexes over the simulation time is observed, indicating the shrinkage of surface area upon binding with Marmin. All other M^{pro}-Ligand complexes and M^{pro} show a comparable behavior till the end of MD simulation. M^{pro}-feruloyltyramine, M^{pro}-Aegelinoside B, M^{pro}-Ervoside exhibit an average SASA value of 130 nm^2 whereas, M^{pro}-Marmin exhibit a lowest average SASA value of 125 nm^2. Trajectory of M^{pro}-Epoxyaurapten complex suggests the highest average SASA (157 nm^2) which indicates the high solvation effect and high molecular size of Epoxyaurapten. Total volume of all systems and M^{pro} lies in between 56 nm^3 to 59 nm^3 and the density lies between 951 g/l to 1200 g/l (SI). Similar volume and density of all systems were seen for other two MD runs. M^{pro}-Marmin, M^{pro}-Epicatechin and M^{pro}-feruloyltyramine show a slight increment of 200 g/l as compared to other M^{pro}-Ligands. In the case of M^{pro} also we observed an increment of 1050 g/l towards the end of the MD.

We have evaluated the interacting residues of protein with six ligands after MD simulations. **Table SI14** indicates the interacting residues of protein with ligands after the MD simulation. Aegelinoside B shows two hydrogen bonds with two pi-alkyl interactions, one anion-pi and one cation-pi interactions. The crucial residues of proteins which involve hydrogen bonds with ligands are, SER46 and GLY143. However, the

docked systems show five hydrogen bonds and the pocket atoms of proteins are changed after MD. In Epoxyaurapten and Marmin no hydrogen bonds could be observed. Interestingly, Ervoside shows seven hydrogen bonds and other non-bonds are pi-sulphur, pi-pi stacked and pi-alkyl interactions. Hydrogen bonds are found in ASN119, ASN142, SER144, SER46, THR24, THR26 and CYC44 with Ervoside ligands (All show H-bond distances less than 3 Å). Epicatechin and Feruloyltyramin exhibit, three and two hydrogen bonds, respectively. Epicatechin exhibits Hydrogen bond interaction with GLU166, GLN192 and GLN189 residues of protein, whereas Feruloyltyramin show hydrogen bond interaction at GLY143 and HIS165 residues of protein. Upon comparing structures of docked systems and systems after MD simulations (**Figure SI13** to **SI17**) it is vividly observable that a slight rearrangement in terms of confirmation of ligands and pockets of proteins occurs in order to interact each of them effectively during the movement.

4. Conclusions

The current study explores the bioactive phytochemicals from four popular herbs for targeting the M^{pro} receptor of SARS-CoV-2 through molecular docking and molecular dynamics studies. Among the 87 phytochemicals chosen for docking study, 6 active phytochemicals can be suggested as the M^{pro} inhibitors based upon the docking score (score > 120 kcal/mol). They are, namely, Ervoside and Feruloyltyramine (from *Aerva lanata*), Epicatechin (from *Biophytum Sensitivum*), Epoxyaurapten, Marmin, and Aegelinoside B (from *Aegle Marmelos*). Aegelinoside B is identified to be the top ranked for docking/binding over the other phytochemicals tested in the current study (Libdock score: 142.50 and binding energy: -8.54 kcal/mol). Based upon the best ranking in terms of dock score values, six ligands were chosen for molecular dynamics simulations for further understanding of structural features such as fluctuations, stability and ligand binding ability, conformational analysis and hydrogen bonds. The interesting results observed in this study paves way for follow up studies on various medicinal herbs found in the locality of the authors and make them familiar to the scientific community. These overlooked herbs have traditionally been used for asthma / bronchitis for years and systematic docking and molecular dynamics studies with M^{pro} will provide the required attention from the international scientific community.

Declarations

Availability of data and materials

All data generated or analyzed during this study are included in supplementary information SI.

Code availability

All docking computations were carried out using BOVIA DISCOVERY STUDIO (version1.8). It is not open-source programs.

Acknowledgement

K S Sandhya thanks Science and Engineering Research Board (SERB), India for the National Post-Doctoral Fellowship (NPDF), award number PDF/2020/001703 and the associated research grant. KSS thanks Dr. Warrier, Mr. Sivakumar (RGBC), Dr. Suveena and Dr. D. Pukazhselvan for the fruitful discussions. KSS also thanks Dr. Meenakshi Sundaram for providing WEBGro server for MD simulations.

Contributions

Sandhya K. S. designed the research, performed virtual screening, docking, analyzed the molecules and wrote the paper. Achuthsankar S. Nair reviewed the manuscript. All authors have read and approved the final manuscript.

Corresponding author

Correspondence to Sandhya K. S. email id drkssandhya@gmail.com

Ethics declarations

Ethics approval

This article does not contain any studies with human or animals performed by any of the authors.

Conflict of interests

All the authors declare that there are no competing interests.

References

1. Yan R, Zhang Y, Li Y et al (2020) Structural basis for the recognition of SARS-CoV-2 by full-length human ACE2. Science 367:1444–1448
2. V'kovski P, Kratzel A, Steiner S et al (2021) Coronavirus biology and replication: implications for SARS-CoV-2. Nat Rev Microbiol 19:155–170
3. Gupta RK (2021) Will SARS-CoV-2 variants of concern affect the promise of vaccines? Nat Rev Immunol 21:340–341
4. Mascola JR, Graham BS, Fauci AS (2021) SARS-CoV-2 viral variants—tackling a moving target. JAMA 325:1261–1262
5. Xie X, Liu Y, Liu J et al (2021) Neutralization of SARS-CoV-2 spike 69/70 deletion, E484K and N501Y variants by BNT162b2 vaccine-elicited sera. Nat Med 27:620–621
6. Kyriakidis NC, López-Cortés A, González EV et al (2021) SARS-CoV-2 vaccines strategies: a comprehensive review of phase 3 candidates. npj Vaccines 6:1–17
7. Moore JP, Offit PA (2021) SARS-CoV-2 vaccines and the growing threat of viral variants. JAMA 325:821–822

8. Mohamed K, Yazdanpanah N, Saghazadeh A, Rezaei N (2021) Computational drug discovery and repurposing for the treatment of COVID-19: a systematic review. Bioorg Chem 106:104490
9. Mouffouk C, Mouffouk S, Mouffouk S et al (2021) Flavonols as potential antiviral drugs targeting SARS-CoV-2 proteases (3CLpro and PLpro), spike protein, RNA-dependent RNA polymerase (RdRp) and angiotensin-converting enzyme II receptor (ACE2). Eur J Pharmacol 891:173759
10. Lockbaum GJ, Reyes AC, Lee JM et al (2021) Crystal structure of SARS-CoV-2 main protease in complex with the non-covalent inhibitor ML188. Viruses 13:174
11. Lu H (2020) Drug treatment options for the 2019-new coronavirus (2019-nCoV). Biosci Trends 14:69–71
12. Wang M, Cao R, Zhang L et al (2020) Remdesivir and chloroquine effectively inhibit the recently emerged novel coronavirus (2019-nCoV) in vitro. Cell Res 30:269–271
13. Odhar HA, Ahjel SW, Albeer AAMA et al (2020) Molecular docking and dynamics simulation of FDA approved drugs with the main protease from 2019 novel coronavirus. Bioinformation 16:236
14. Dotolo S, Marabotti A, Facchiano A, Tagliaferri R (2021) A review on drug repurposing applicable to COVID-19. Brief Bioinform 22:726–741
15. Rismanbaf A (2020) Potential treatments for COVID-19; a narrative literature review.Archives of academic emergency medicine8
16. Tarighi P, Eftekhari S, Chizari M et al (2021) A review of potential suggested drugs for coronavirus disease (COVID-19) treatment. Eur J Pharmacol 895:173890
17. Goswami T, Bagchi B (2020) Molecular docking study of receptor binding domain of SARS-CoV-2 Spike Glycoprotein with Saikosaponin, a triterpenoid natural product
18. Bouchentouf S, Missoum N (2020) Identification of Compounds from Nigella Sativa as New Potential Inhibitors of 2019 Novel Coronasvirus (Covid-19). Molecular Docking Study
19. Warrier PK (1993) Indian medicinal plants: a compendium of 500 species. Orient Blackswan
20. Sarkar T, Salauddin M, Hazra SK, Chakraborty R (2020) A novel data science application approach for classification of nutritional composition, instrumental colour, texture and sensory analysis of bael fruit (Aegle marmelos (L) correa). Int J Intell Networks 1:59–66
21. Mariswamy Y, Gnaraj WE, Johnson M (2011) Chromatographic finger print analysis of steroids in Aerva lanata L by HPTLC technique. Asian Pac J Trop Biomed 1:428–433
22. Ajithkumar D, Seeni S (1998) Rapid clonal multiplication through in vitro axillary shoot proliferation of Aegle marmelos (L.) Corr., a medicinal tree. Plant Cell Rep 17:422–426
23. Arumugam G, Sinniah UR, Swamy MK, Lynch PT (2020) Micropropagation and essential oil characterization of Plectranthus amboinicus (Lour.) Sprengel, an aromatic medicinal plant. In Vitro Cellular & Developmental Biology-Plant 56:491–503
24. Baliga MS, Bhat HP, Joseph N, Fazal F (2011) Phytochemistry and medicinal uses of the bael fruit (Aegle marmelos Correa): A concise review. Food Res Int 44:1768–1775

25. Singh G, Singh OP, Prasad YR et al (2002) Studies on essential oils, Part 33: chemical and insecticidal investigations on leaf oil of Coleus amboinicus Lour. Flavour Fragr J 17:440–442
26. Chowdhury D, Sayeed A, Islam A et al (2002) Antimicrobial activity and cytotoxicity of Aerva lanata. Fitoterapia 73:92–94
27. Khare CP (2008) Indian medicinal plants: an illustrated dictionary. Springer Science & Business Media
28. Sakthivel KM, Guruvayoorappan C (2012) Biophytum sensitivum: Ancient medicine, modern targets. J Adv Pharm Tech Res 3:83
29. DISCOVERY (2018) Dassault systems, San Diego
30. Hastings J, Owen G, Dekker A et al (2016) ChEBI in 2016: Improved services and an expanding collection of metabolites. Nucleic Acids Res 44:D1214–D1219. https://doi.org/10.1093/nar/gkv1031
31. Kim S, Chen J, Cheng T et al (2021) PubChem in 2021: new data content and improved web interfaces. Nucleic Acids Res 49:D1388–D1395. https://doi.org/10.1093/nar/gkaa971
32. Jia C-Y, Li J-Y, Hao G-F, Yang G-F (2020) A drug-likeness toolbox facilitates ADMET study in drug discovery. Drug Discovery Today 25:248–258
33. Veber DF, Johnson SR, Cheng H-Y et al (2002) Molecular properties that influence the oral bioavailability of drug candidates. J Med Chem 45:2615–2623
34. Guedes IA, Costa LSC, dos Santos KB et al (2021) Drug design and repurposing with DockThor-VS web server focusing on SARS-CoV-2 therapeutic targets and their non-synonym variants. Sci Rep 11:1–20
35. Oostenbrink C, Villa A, Mark AE, van Gunsteren WF (2004) A biomolecular force field based on the free enthalpy of hydration and solvation: the GROMOS force-field parameter sets 53A5 and 53A6. J Comput Chem 25:1656–1676
36. Vatansever EC, Yang K, Kratch KC et al (2020) Bepridil is potent against SARS-CoV-2 In Vitro. bioRxiv: the preprint server for biology 2020.05.23.112235. https://doi.org/10.1101/2020.05.23.112235
37. Liu W-S, Li H-G, Ding C-H et al (2021) Screening potential FDA-approved inhibitors of the SARS-CoV-2 major protease 3CL(pro) through high-throughput virtual screening and molecular dynamics simulation. Aging 13:6258–6272. https://doi.org/10.18632/aging.202703
38. Götte M (2021) Remdesivir for the treatment of Covid-19: the value of biochemical studies. Curr Opin Virol 49:81–85. https://doi.org/https://doi.org/10.1016/j.coviro.2021.04.014
39. Yuce M, Cicek E, Inan T et al (2021) Repurposing of FDA-approved drugs against active site and potential allosteric drug-binding sites of COVID-19 main protease. Proteins Struct Funct Bioinform 89:1425–1441. https://doi.org/https://doi.org/10.1002/prot.26164
40. Ray AK, sen Gupta PS, Panda SK et al (2022) Repurposing of FDA-approved drugs as potential inhibitors of the SARS-CoV-2 main protease: Molecular insights into improved therapeutic discovery. Comput Biol Med 142:105183. https://doi.org/https://doi.org/10.1016/j.compbiomed.2021.105183

41. Macip G, Garcia-Segura P, Mestres-Truyol J et al (2022) Haste makes waste: A critical review of docking-based virtual screening in drug repurposing for SARS-CoV-2 main protease (M-pro) inhibition. Med Res Rev 42:744–769. https://doi.org/https://doi.org/10.1002/med.21862
42. Kumar Y, Singh H, Patel CN (2020) In silico prediction of potential inhibitors for the main protease of SARS-CoV-2 using molecular docking and dynamics simulation based drug-repurposing. J Infect Public Health 13:1210–1223. https://doi.org/https://doi.org/10.1016/j.jiph.2020.06.016
43. Umadevi P, Manivannan S, Fayad AM, Shelvy S (2020) In silico analysis of phytochemicals as potential inhibitors of proteases involved in SARS-CoV-2 infection.Journal of Biomolecular Structure and Dynamics1–9
44. Goyal M, Pareek A, Nagori BP, Sasmal D (2011) Aerva lanata: A review on phytochemistry and pharmacological aspects. Pharmacogn Rev 5:195
45. Gu Y-Y, Zhang M, Cen H et al (2021) Quercetin as a potential treatment for COVID-19-induced acute kidney injury: Based on network pharmacology and molecular docking study. PLoS ONE 16:e0245209
46. Hiremath S, Kumar HD, Nandan M et al (2021) In silico docking analysis revealed the potential of phytochemicals present in Phyllanthus amarus and Andrographis paniculata, used in Ayurveda medicine in inhibiting SARS-CoV-2. 3 Biotech 11:1–18
47. Chang CW, Hsu FL, Lin JY (1994) Inhibitory effects of polyphenolic catechins from Chinese green tea on HIV reverse transcriptase activity. J Biomed Sci 1:163–166
48. Gour A, Manhas D, Bag S et al (2021) Flavonoids as potential phytotherapeutics to combat cytokine storm in SARS-CoV-2. Phytother Res 35:4258–4283
49. Ghosh R, Chakraborty A, Biswas A, Chowdhuri S (2021) Evaluation of green tea polyphenols as novel corona virus (SARS CoV-2) main protease (Mpro) inhibitors–an in silico docking and molecular dynamics simulation study. J Biomol Struct Dynamics 39:4362–4374
50. Arumugam G, Swamy MK, Sinniah UR (2016) Plectranthus amboinicus (Lour.) Spreng: botanical, phytochemical, pharmacological and nutritional significance. Molecules 21:369
51. Bhatt P, Joseph GS, Negi PS, Varadaraj MC (2013) Chemical composition and nutraceutical potential of Indian borage (Plectranthus amboinicus) stem extract.Journal of Chemistry2013
52. Maste MM, Saxena A (2020) Screening of Plectranthus amboinicus against COVID-19 coronavirus-in silico approach. J Appl Pharm Sci 10:90–97
53. Hashida M (2020) Role of pharmacokinetic consideration for the development of drug delivery systems: A historical overview. Adv Drug Deliv Rev 157:71–82
54. Bhardwaj VK, Singh R, Sharma J et al (2021) Identification of bioactive molecules from tea plant as SARS-CoV-2 main protease inhibitors. J Biomol Struct Dynamics 39:3449–3458
55. Štekláč M, Zajaček D, Bučinský L (2021) 3CLpro and PLpro affinity, a docking study to fight COVID19 based on 900 compounds from PubChem and literature. Are there new drugs to be found? J Mol Struct 1245:130968

56. Sharma A, Vora J, Patel D et al (2020) Identification of natural inhibitors against prime targets of SARS-CoV-2 using molecular docking, molecular dynamics simulation and MM-PBSA approaches.Journal of Biomolecular Structure and Dynamics1–16
57. Chowdhury P (2021) In silico investigation of phytoconstituents from Indian medicinal herb ‘Tinospora cordifolia (giloy)’against SARS-CoV-2 (COVID-19) by molecular dynamics approach. J Biomol Struct Dynamics 39:6792–6809
58. Khan SA, Zia K, Ashraf S et al (2021) Identification of chymotrypsin-like protease inhibitors of SARS-CoV-2 via integrated computational approach. J Biomol Struct Dynamics 39:2607–2616
59. Khan MT, Ali A, Wang Q et al (2021) Marine natural compounds as potents inhibitors against the main protease of SARS-CoV-2—a molecular dynamic study. J Biomol Struct Dynamics 39:3627–3637
60. Alazmi M, Motwalli O (2021) In silico virtual screening, characterization, docking and molecular dynamics studies of crucial SARS-CoV-2 proteins. J Biomol Struct Dynamics 39:6761–6771

Figures

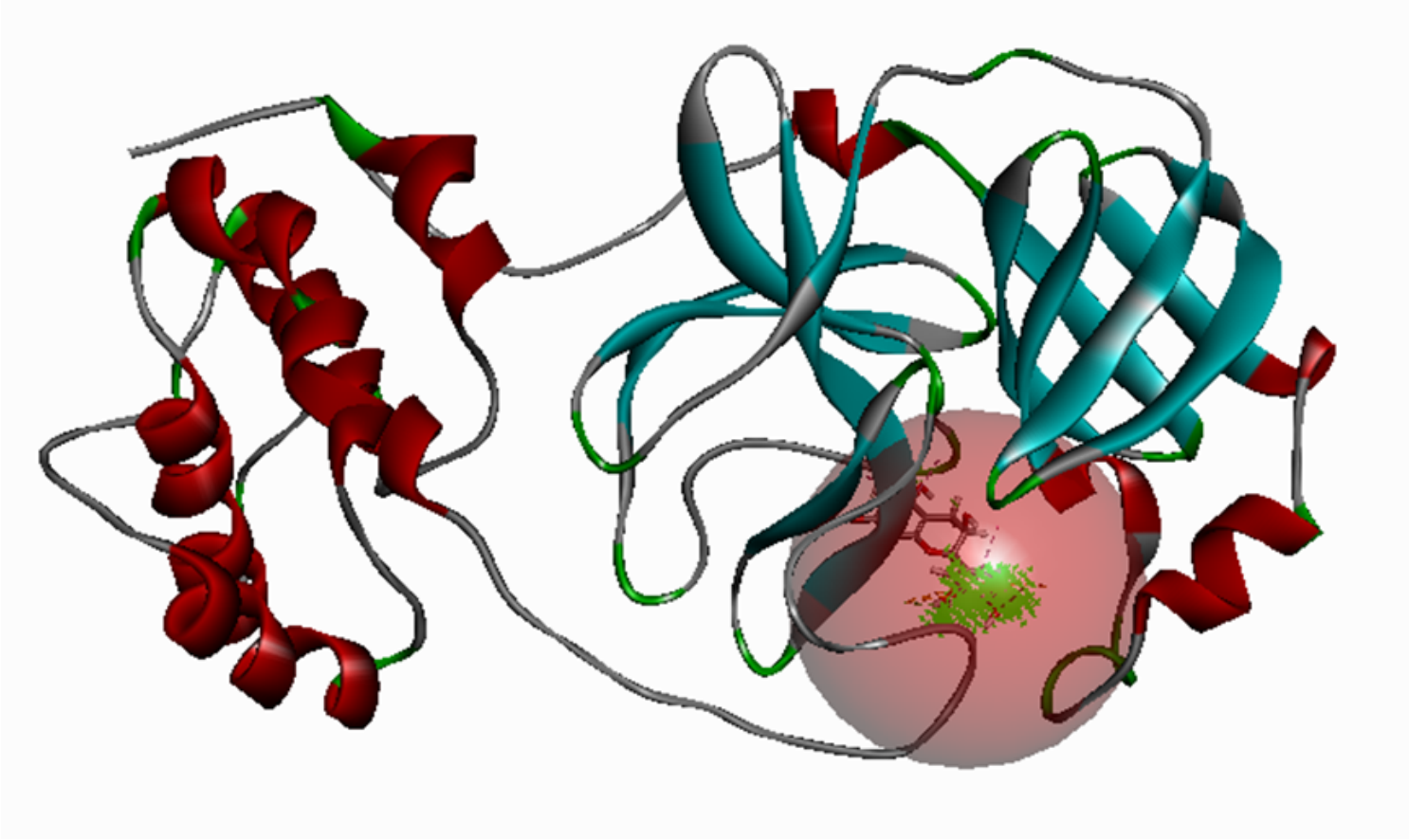

Figure 1

Position of an active binding transparent site (radius of 10 Å) centred at 12.355 14.273 71.259 XYZ coordinates in M^{pro}. A representative example of ligand is docked inside the binding active site.

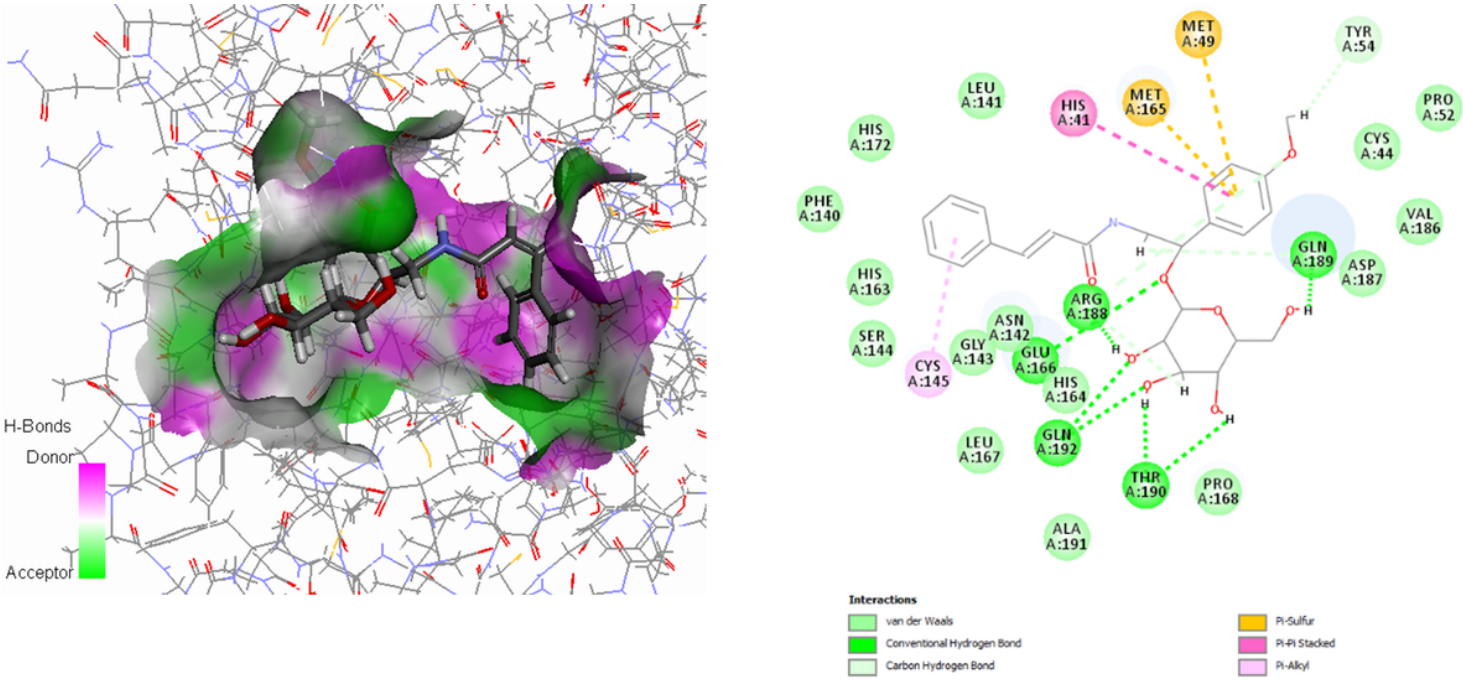

Figure 2

A) 3D interaction diagram with a surface color by hydrogen bond type B) 2D interaction diagram of Aegelinoside B with M^{pro}.

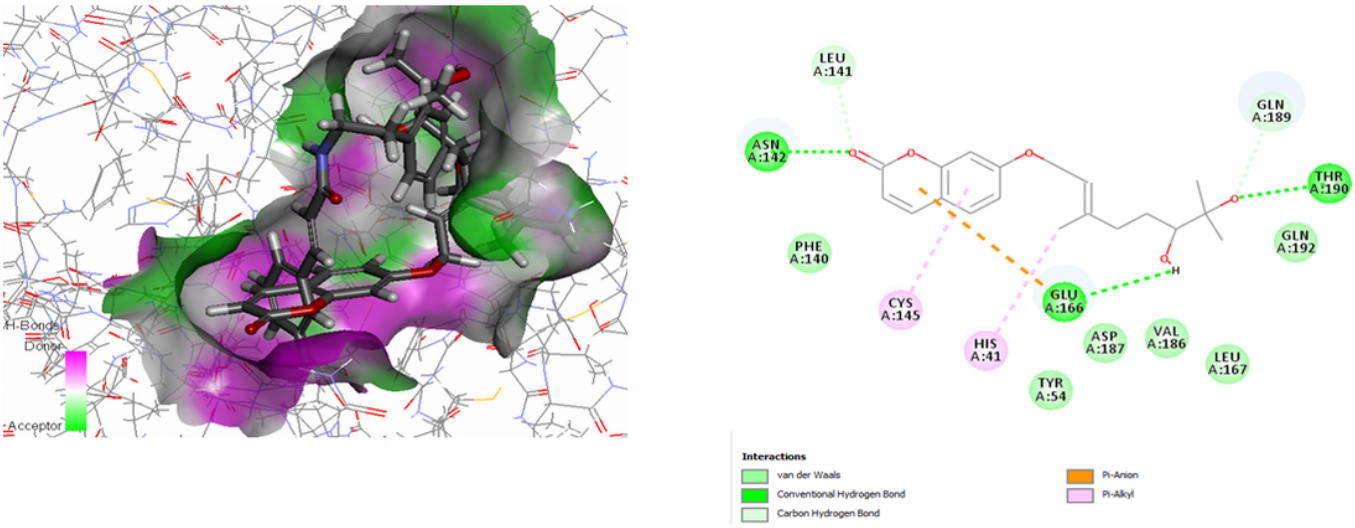

Figure 3

A) 3D interaction diagram with a surface color by hydrogen bond type B) 2D interaction diagram of Epoxyaurapten with M^{pro}.

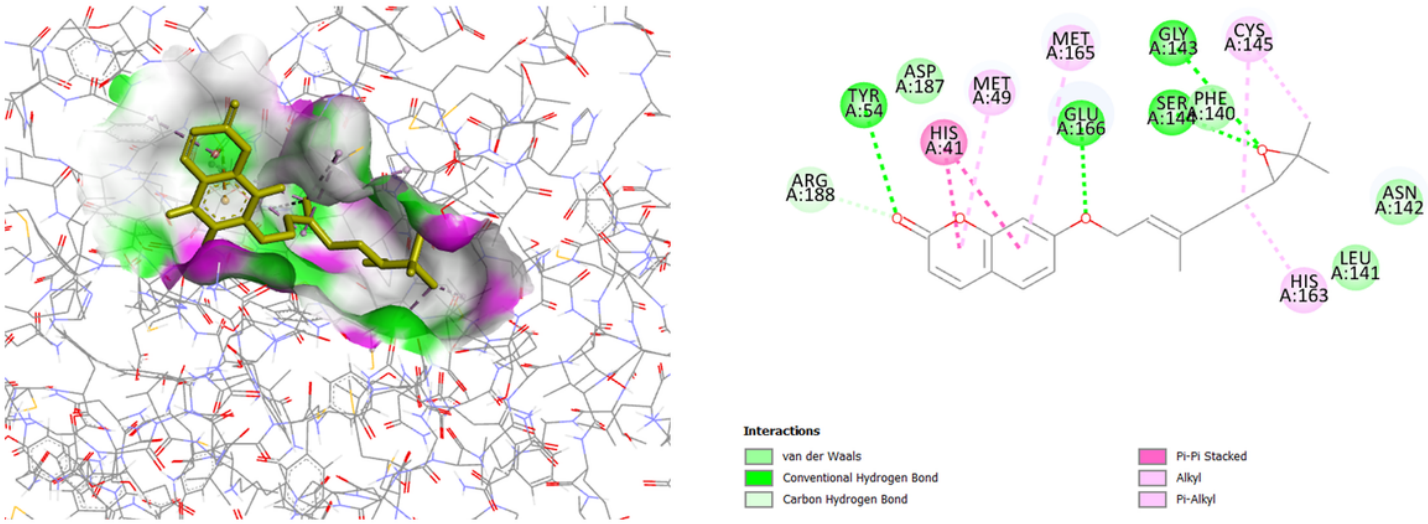

Figure 4

A) 3D interaction diagram with a surface color by hydrogen bond type B) 2D interaction diagram of Marmin with M^{pro}

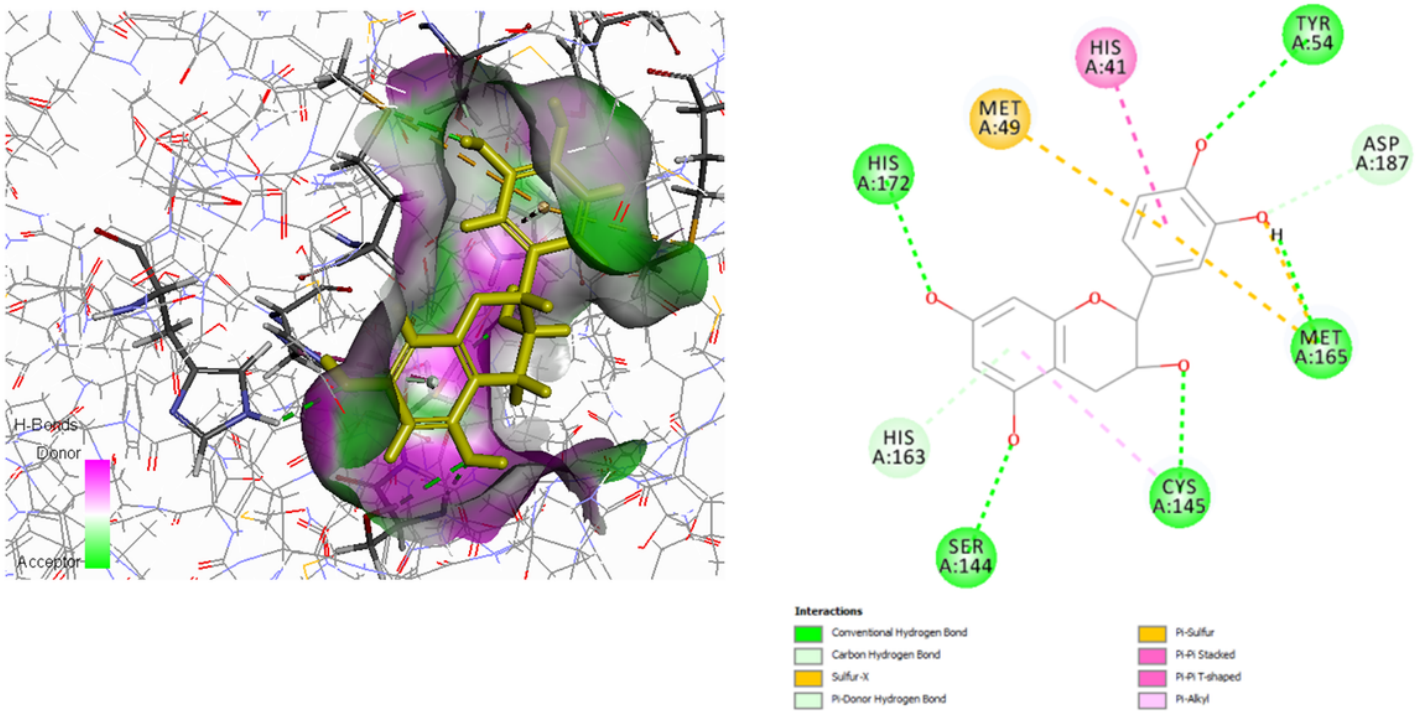

Figure 5

A) 3D interaction diagram with a surface color by hydrogen bond type B) 2D interaction diagram of Ervoside with M^{pro}.

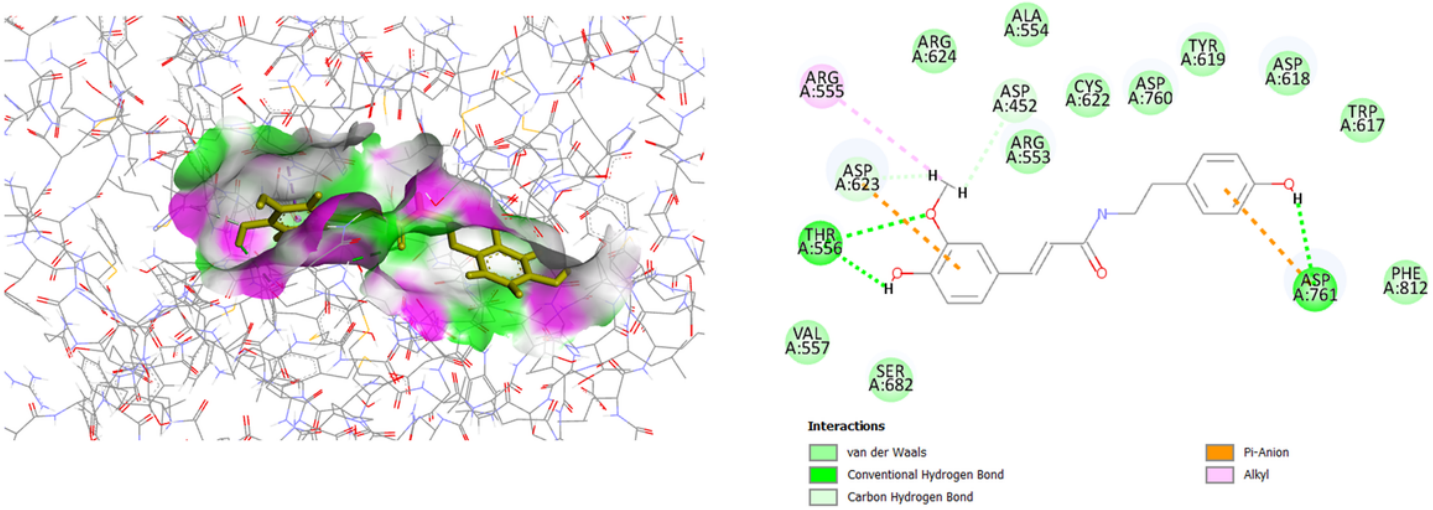

Figure 6

A) 3D interaction diagram with a surface color by hydrogen bond type B) 2D interaction diagram of Feruloyltyramine with M^{pro}

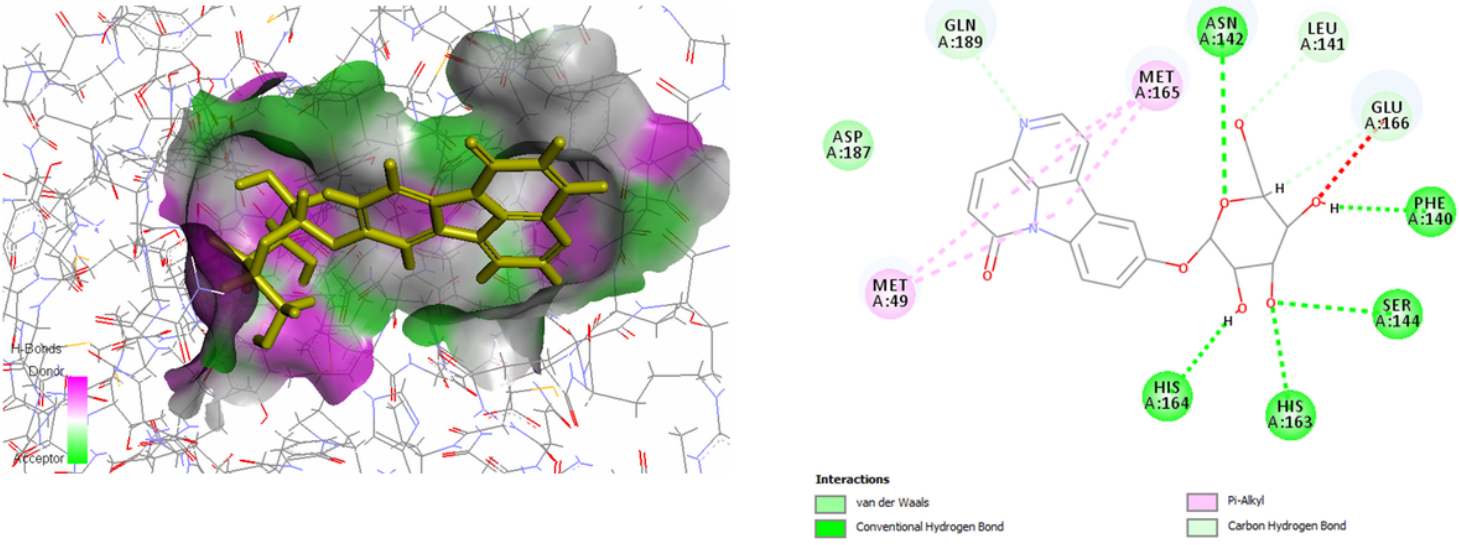

Figure 7

A) 3D interaction diagram with a surface color by hydrogen bond type B) 2D interaction diagram of Epicatechin with M^{pro}

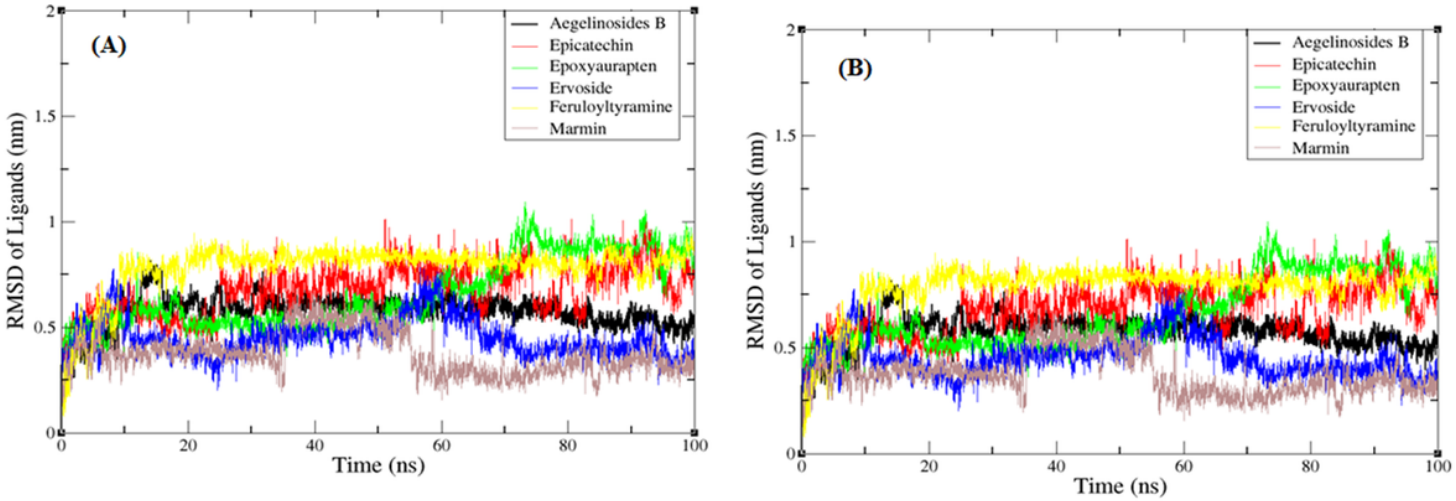

Figure 8

RMSD profile of A) M^{pro}-Ligands and B) Ligands.

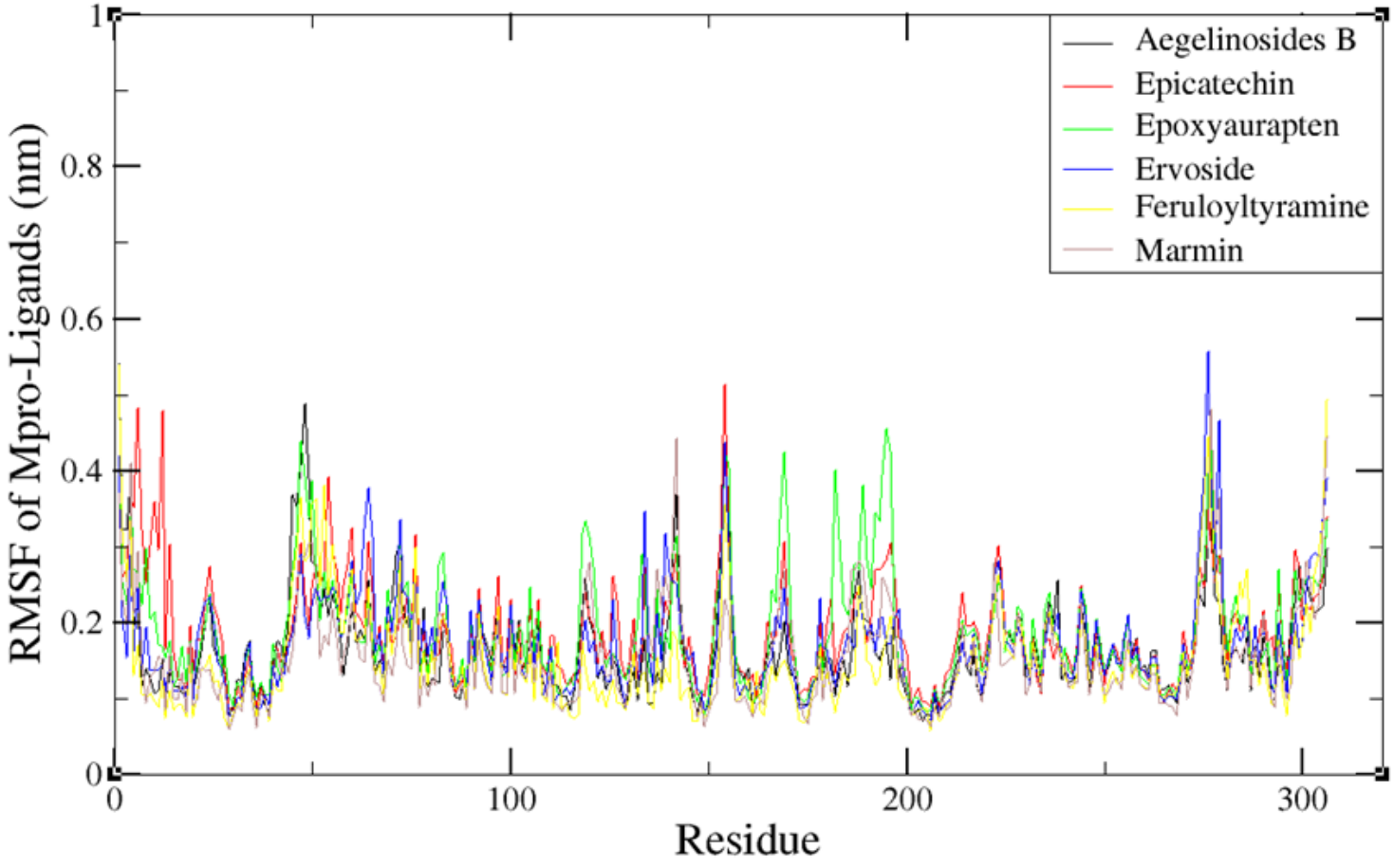

Figure 9

RMSF of M^{pro}-Ligands.

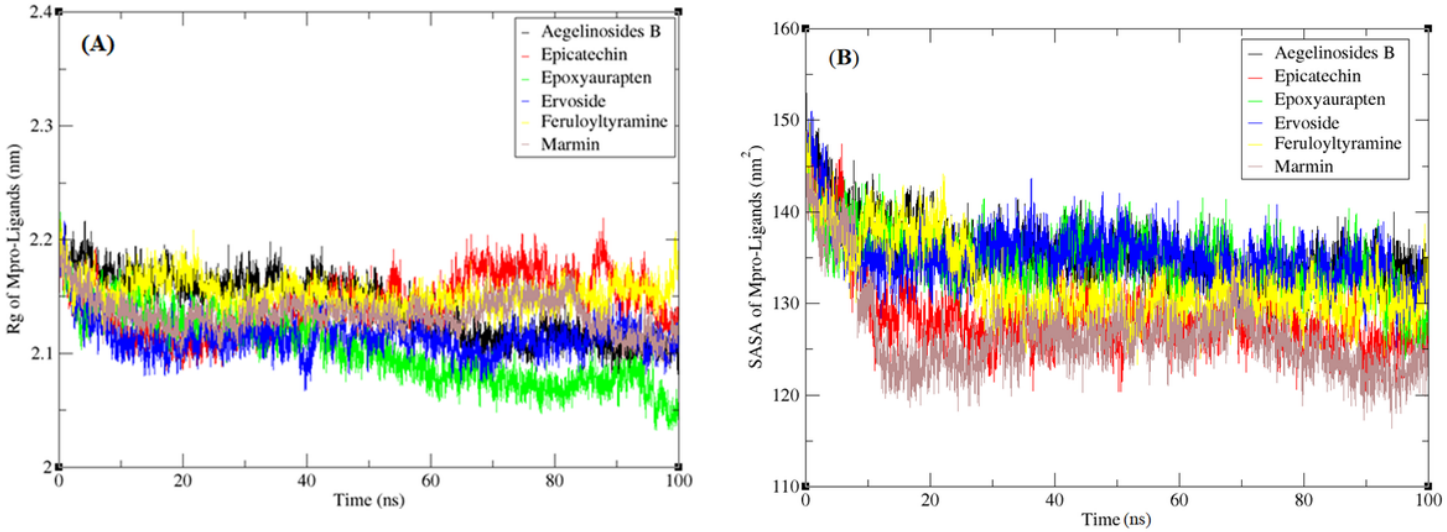

Figure 10

Rg and SASA of M^{pro}-Ligands and M^{pro}.

Supplementary Files

This is a list of supplementary files associated with this preprint. Click to download.

- Graphicalabstract.png
- Moleculardynamicsanddockingstudiesonpotentially1SI.doc